The Cryosphere Discuss., doi:10.5194/tc-2016-112, 2016
Manuscript under review for journal The Cryosphere
Published: 6 June 2016
© Author(s) 2016. CC-BY 3.0 License.

The Cryosphere Discussions

Benefits of assimilating thin sea-ice thickness from SMOS-Ice into the TOPAZ system

Jiping Xie[1], Francois Counillon[1], Laurent Bertino[1], XiangshanTian-Kunze[2], and Lars Kaleschke[2]

1. Nansen Environmental and Remote Sensing Center, Bergen, Norway
2. Institute of Oceanography, University of Hamburg, German

The Cryosphere Discuss., doi:10.5194/tc-2016-112, 2016
Manuscript under review for journal The Cryosphere
Published: 6 June 2016
© Author(s) 2016. CC-BY 3.0 License.

Abstract

An observation product for thin sea ice thickness (SMOS-Ice) is derived from the brightness temperature data of the European Space Agency's (ESA) Soil Moisture and Ocean Salinity (SMOS) Mission, and available in real-time at daily frequency during the winter season. In this study, we investigate the benefit of assimilating SMOS-Ice into the TOPAZ system. TOPAZ is a coupled ocean-sea ice forecast system that assimilates SST, altimetry data, temperature and salinity profiles, ice concentration, and ice drift with the Ensemble Kalman Filter (EnKF). The conditions for assimilation of sea ice thickness thinner than 0.4m are favorable, as observations are reliable below this threshold and their probability distribution is comparable to that of the model. Two paralleled runs of TOPAZhave been performed respectively in March and November 2014, with assimilation of thin sea ice thickness (thinner than 0.4 m) in addition to the standard ice and ocean observational data sets. It is found that the RMSD of thin sea-ice thickness is reduced by 11% in March and 22% in November suggesting that SMOS-Ice has a larger impact during the beginning of freezing season. There is a slight improvementof the ice concentration and no degradation of the ocean variables. The Degrees of Freedom for Signal (DFS) indicate that the SMOS-Ice contents important information (> 20% of the impact of all observations)for some areas in the Arctic. The areas of largest impact are the Kara Sea, the Canadian archipelago, the Baffin Bay, the Beaufort Sea and the Greenland Sea. This study suggests that SMOS-Ice is a good complementary dataset that can be safely included in the TOPAZ system as it improves the ice thickness and the ice concentration but does not degrade other quantities.

Keywords: SMOS-Ice; EnKF; OSE; thin sea-ice thickness; DFS;

The Cryosphere Discuss., doi:10.5194/tc-2016-112, 2016
Manuscript under review for journal The Cryosphere
Published: 6 June 2016
© Author(s) 2016. CC-BY 3.0 License.

1. Introduction

The Arctic climate system has undergone large changes during the last 20 years: increase of temperature (Chapman and Walsh, 1993; Serreze et al., 2000; Karl et al., 2015; Roemmich et al., 2015), decrease of sea ice extent (Chapman and Walsh, 1993; Johannessen et al., 1999; Shimada et al., 2006;), sea ice thinning and loss of sea ice volume (Rothrock et al., 1999; Kwok and Rothrock, 2009; Laxon et al., 2013). The interpretation of such changes is severely hampered by the sparseness and the deversity of observational network. The reanalysis database that combines the sparse observations with dynamically consistent modeling is becoming an important tool.

While observations of sea ice concentrations have been available for the past 30 years, observations of sea ice thickness are comparatively sparse. An improved knowledge of the ice thickness would be greatly beneficial both for model developments and for improving the accuracy of operational ocean forecasting system.The initialization of sea-ice thickness is also expected to improve predictability on seasonal time scale (Guemas et al. 2014). Until the last decade, observations of sea-ice thickness were mostly limited to field campaigns or submarine measurements. Major efforts in remote sensing have been proposed to monitor the spatiotemporal evolution of ice thickness, and gradually obtained vairious products from different satellite retrieval algorithms. Measurements of thick sea ice draft on basin-wide scales have been derived from laser altimeters on board ICESat (e.g., Forsberg and Skourup, 2005; Kurtz et al., 2009; Kwok and Rothrock, 2009) or from radar altimeters on ERS, EnviSAT and CryoSat2 (e.g., Laxon et al., 2003; Giles et al., 2008; Connor et al., 2009). Still large uncertainties remain in the accuracy of the resulting ice thickness estimates (larger than 0.5 m) due to uncertainties in the snow depth and the sea ice density (Zygmuntowska et al., 2014). A new database based on Cryostat-2 has been provided (Laxon 2013; Ricker et al., 2014) and has been made available in near real time (Tilling et al. 2016). Finally, methods for sea ice thickness retrieval based on measurements of the brightness temperature at a low microwave frequency of 1.4 GHz (L-band: wavelength λ_a=21 cm) have been developed in preparation for the European Space Agency's (ESA) Soil Moisture and Ocean Salinity (SMOS) mission (Heygster et

© Author(s) 2016. CC-BY 3.0 License.

al., 2009; Kaleschke et al., 2010). It has been shown that SMOS can be used to retrieve level ice thickness up to half a meter under cold conditions (Kaleschke et al., 2012; Huntemann el al., 2014).

An improved retrieval method based on a radiative transfer model and a thermodynamic sea ice model has been further proposed by considering the variations of ice temperature, salinity and a statistical thickness distribution (Tian-Kunze et al., 2014). The operational daily product derived using this method, henceforth called SMOS-Ice, has been validated during a field campaign in the Barents Sea (Kaleschke et al., 2016; Mecklenburg et al., 2016) and will be used in this study. Aiming at the operational application of the thickness measurements for sea ice, the SMOS-Ice data contain daily products of sea ice thickness since the winter of 2010 (Tian-Kunze et al., 2014). Yang et al. (2015) studied the benefit of SMOS-Ice during the freezing period, with the LSEIK (an assimilation methodrelated to the EnKF) in a nested Arctic configuration of the MITgcm. They found that SMOS-Ice leads to improvement of ice thickness and ice concentration. This study is a follow up and assess: 1) the impact of assimilating SMOS-Ice both during the beginnings of melting and freezing seasons; 2) the relative contribution of SMOS-ice compared to a complete set of observationstypically used in a state of the art forecasting system.

The TOPAZ system is a coupled ocean-sea ice data assimilation system that focuses on the marine environment in the Arctic region. It is the operational Arctic forecast system in the Copernicus Marine Services (http://marine.copernicus.eu/). The system provides 10-days coupled physical-biogeochemical forecast every day and long-term reanalysis (Sakov et al., 2012; Lien et al., 2016; Xie et al., 2016). At present, the TOPAZ system assimilates the Sea Surface Temperature (SST), along-track Sea Level Anomalies (SLA) from satellite altimeters, in situ temperature and salinity profiles, Sea Ice Concentration (ICEC) and sea ice drift data from satellites with the Ensemble Kalman Filter (EnKF). The reanalysis product of the TOPAZ system has been widely used in studies about ocean circulation and sea ice in the northern Atlantic Ocean or in the Arctic region (Melsom et al., 2012; Johannessen et al., 2014; Korosov et al., 2015; Lien et al., 2016). However, TOPAZ does not assimilate sea ice thickness, and does not apply postprocess

© Author(s) 2016. CC-BY 3.0 License.

for this variable. In the Arctic reanalysis, the daily sea ice thickness of TOPAZ for the period 1991-2013 has been validated and compared to the observations from ICESat and IceBridge in Xie et al. (submitted in 2016). While the spatial pattern and regression compare reasonably well, the large biases exist. Inaccuracy in the ice thickness is a drawback of coupled ice-ocean models in the Arctic (Johnson et al., 2012; Smith et al., 2015).

This paper is organized as follows: section 2 introduces the main components of TOPAZ system including the model, the assimilation scheme, and the observations assimilated. In section 3, we compare SMOS-ice data to the TOPAZ reanalysis for the period 2010-2013, to investigate potential biases and whether conditions are favorable for data assimilation. In section 4, an Observing System Experiment (OSE) is conducted, consisting of two assimilation runs with and without assimilating the SMOS-Ice data during 2014. In Section 5, we comparedthe contributions of SMOS-Ice relative to other types of observations.

2. Descriptions of TOPAZ data assimilation system

2.1 The coupled ice-ocean model

The ocean general circulation model used in the TOPAZ system is the version 2.2 of the Hybrid Coordinate Ocean Model (HYCOM) developed at University of Miami (Bleck, 2002; Chassignet et al., 2003). HYCOM uses a hybrid vertical coordinate, which smoothly transits from isopycnal layers in the stratified open ocean to z-level coordinates in the unstratified surface mixed layer. This feature has been demonstrated in a wide range of applications from the deep oceans to the shelf (Winther and Evensen, 2006; Chassignet et al., 2009). The NERSC-HYCOM model is coupled to a sea-ice model for which the ice thermodynamics are described in Drange and Simonsen (1996) and theice dynamics are based on the elastic-viscous-plastic rheology described in Hunke and Dukowicz (1997) and with a modification from Bouillon et al. (2013). TOPAZ uses conformal mapping (Bentsen et al., 1999) and has a quasi-homogeneous horizontal resolution of 12-16 km in the Arctic as shown in Fig. 1.

The Cryosphere Discuss., doi:10.5194/tc-2016-112, 2016
Manuscript under review for journal The Cryosphere
Published: 6 June 2016
© Author(s) 2016. CC-BY 3.0 License.

The temperature and salinity at model lateral boundaries are relaxed to a combined climatology between the World Atlas of 2005 (WOA05, Locarnini et al., 2006) and the version 3.0 of the Polar Science Center Hydrographic Climatology (PHC, Steele et al., 2001). A seasonal inflow from the Pacific Ocean through the Bering Strait is imposed, which amplitude is following the observations from Woodgate et al. (2012).

2.2 Implementation of the EnKF in TOPAZ

The analysis field of model state at time of t_i, is expressed as follows:

$$\mathbf{X}_i^a = \mathbf{X}_i^f + \mathbf{K}_i(\mathbf{y}_i - \mathbf{H}_i\mathbf{X}_i^f) \quad (1).$$

Where $\mathbf{X_i}$ is the model state vector, the superscripts “a” and “f” refer to the analysis and the forecast respectively. The ensemble consists of 100 dynamical members. $\mathbf{H_i}$ is the observation operator and $\mathbf{y_i}$ is the observation vector, which includes all observations at the assimilation time window. The Kalman gain $\mathbf{K_i}$ in Equation (1) is calculated as:

$$\mathbf{K}_i = \mathbf{P}_i^f\mathbf{H}_i^T[\mathbf{H}_i\mathbf{P}_i^f\mathbf{H}_i^T + \mathbf{R}_i]^{-1} \quad (2).$$

Where $\mathbf{R_i}$ is the matrix of observation error variance, and $\mathbf{P_i}$ is the matrix of background error covariance. The TOPAZ system uses the deterministic EnKF (DEnKF, Sakov and Oke, 2008; Sakov et al., 2012), which is a square-root filter implementation of the EnKF. The covariance $\boldsymbol{P}^a$ is equal to

$$\mathbf{P}_i^a = (\mathbf{I} - \mathbf{K}_i\mathbf{H}_i)\mathbf{P}_i^f + \frac{1}{4}\mathbf{K}_i\mathbf{H}_i\mathbf{P}_i^f\mathbf{H}_i\mathbf{K}_i^T \quad (3)$$

Compared to the traditional estimation of the analyzed error covariance, the extra term is quadratic and positive. It induces an overestimation of the analyzed error covariance,which partially compensates the need for ensemble inflation.

An overview of the observations assimilated in the present TOPAZ system is given in Table 1 (see as well Sakov et al, 2012; Xie et al., submit in 2016). Observations are quality controlled and superobed as in Sakov et al (2012). The system assimilates the following data set on a weekly basis: the gridded OSTIA SST (Donlon et al., 2012); OSI-SAF ice concentration available for the analysis day; along-track SLA; delayed-mode profiles of temperature and salinity, and the sea-ice drift during the 2 days prior to the analysis. All

© Author(s) 2016. CC-BY 3.0 License.

measurements are retrieved from http://marine.copernicus.eu. SLA data and sea ice drift are assimilated asynchronously as described in Sakov et al. (2010)

3. Bias analyses for thin ice thickness in TOPAZ

TOPAZ provides a reanalysis at daily frequency of physical variables including sea ice thickness, which was validated by in situ and satellite observations in Xie et al. (2016). An assumption made for data assimilation is that the model and observations have unbiased mean and uncertainties estimates. Therefore, we investigate in this section the biases in the thickness of thin sea ice during four winters from 2010-2014.

SMOS-Ice products are available since 2010 in the winter months, from 15th October to 15th April. Figure 2 shows the TOPAZ ice thickness as conditional expectations with respect to SMOS-Ice data organized by bin of 5 cm. The TOPAZ equivalent ice thickness is calculated at observations location and time. The error bars show the observation uncertainty (in red) and the TOPAZ RMSD (in cyan) compared to the observations of the bin. Overall, the sea ice thickness in TOPAZ tends to be overestimated. However, the comparison varies largely form month to monthand as a function of ice thickness, especially for thick ice. As an example, the model overestimates the high thickness values (>0.4 m) during October. However, during November the model underestimates the high thickness values (>0.4 m), while it largely overestimates them in Feb-Apr. For thicknesses lower than 0.4 m, the match between the observations and the simulations of TOPAZ is closer and more consistent through the winter season and in consecutive bins.There is no clear bias from October–December but an increasing thick bias from January-April. There is a priori no indication whether the bias is a model bias or an observation bias. In order to avoid multivariate transfers of bias, whichever the source, the assimilation of SMOS-Ice is restrained to thicknessless than 0.4 m. This is also motivated by physical considerations on the wavelength of L-Band microwaves. The penetration depth into sea ice is about 0.5 m at this microwave frequency (Kaleschke et al., 2010; Huntemann et al., 2014), and the effect of ice melting may lead to a saturation thickness of less than 0.4 m, (see Heygster et al. (2009)).

The Cryosphere Discuss., doi:10.5194/tc-2016-112, 2016
Manuscript under review for journal The Cryosphere
Published: 6 June 2016
© Author(s) 2016. CC-BY 3.0 License.

The Cryosphere Discussions

Furthermore, relative to the thickness observations of SMOS-Ice for the thin sea ice no more than 0.4 m, the yearly bias in the period 2010-2014 are shown by the black lines in Fig. 3. After 2011, the thick bias is increased, and reaches about 0.1 m in 2014. The thick bias in March is also found lagerthan that in November. Also the spatial variability of the bias is shown in the right panel of Fig.3, with the bias being largest in the Beaufort Sea and in the Kara Sea. In 2014, there is a thick bias in all regions.

4. Observing System Experiment of SMOS-Ice

4.1 Design of OSE runs for the SMOS-Ice

The SMOS-Ice ice thickness data (version 2.1) is gridded at a resolution of approximately 12.5 km and available at daily frequency in winter months. Only the observations between 0 and 0.4 m, with a distance of at least 30 km away from the coast, are used (See Section 3). The innovations in Equation (1) are expressed as a sea ice volume, which is an additive variable suited for spatial interpolation:

$$\mathbf{\Delta hice} = \mathbf{y}_{\mathbf{smos}} - \mathbf{H}_{\mathbf{i}}(\mathbf{h}_{\mathrm{mod}} \times \mathbf{f}_{\mathbf{mod}}) \qquad (4)$$

where **H** is the bilinear interpolation, h_{mod} and f_{mod} are the model sea ice thickness and concentration respectively. To highlight the additional impacts of observations, two assimilation runs for Observing System Experiment (OSE) are named as follows:

-Official Run: usesthe standard observational network of the TOPAZ system. It assimilates weekly the along-track SLA (TSLA), SST, in situ profiles of temperature and salinity, sea-ice concentrations and sea-ice drift data (listed in **Table** 1).

-Test Run: assimilates SMOS-Ice data (version 2.1) in addition to observations assimilated in the official run. The observation error standard deviation of the sea ice thickness uses the uncertainties recommended by the provider, with an upper limit of 5 m beyond which the observations are assumed to have negligible impacts. The observation error is assumed spatially uncorrelated.

© Author(s) 2016. CC-BY 3.0 License.

We have two parallel assimilation runs focusing on two typical time periods within the beginnings of ice melting and freezing, from 19th February to 31th March and from 22th October to 30th November in 2014. Both runs are driven by the same atmospheric high frequency forcing from ERA-Interim (Simmons et al., 2007; Dee et al., 2011). Finally, the daily averaged outputs in March and November are used for the evaluation.

4.2 Error analysis in the OSE runs

The analysis focuses on the following target quantities as listed in Table 1: sea ice thickness (from SMOS-Ice), sea ice concentration, SST and SLA. All quantities are calculated from daily averages, and we calculate the bias and the RMSD:

$$\mathbf{Bias} = \frac{1}{\mathbf{N}}\sum_{i=1}^{\mathbf{N}}(\mathbf{H}_i\overline{\mathbf{X}}_i^f - \mathbf{y}_i) \tag{5}$$

$$\mathbf{RMSD} = \sqrt{\frac{1}{\mathbf{N}}\sum_{i=1}^{\mathbf{N}}(\mathbf{H}_i\overline{\mathbf{X}}_i^f - \mathbf{y}_i)^2}, \tag{6}$$

where $\overline{\mathbf{X}}_i^f$ is the daily averaged forecast of the model variables, which is compared to the observation on the same location and time.

The spatial distribution of selected SMOS-Ice data for thin sea ice is shown in the top panels of Fig. 4during March and November of 2014. In March, the available observations in the Beaufort Sea are very few, and inhomogeneously distributed - mainly located in the coastal esturay areas. Therefore in the following analysis, we will only present the result in the Beaufort Sea for November. In the middle panels of Fig. 4, the differences of RMSD for sea-ice thickness between the **Official Run** and the **Test Run** are shown (red color indicates an improvement due to assimilation of SMOS-Ice). In March, the improvements are mainly found to the east of Franz Josef Land and to some extent near the ice edge in the Greenland Sea. In November, the reduction of RSMD is larger than 0.2 m in the Beaufort Sea, the Greenland Sea and to the north of Svalbard. Finally, the differences of monthly ice thickness between the **Official Run** and the **Test Run** are shown in the

The Cryosphere Discuss., doi:10.5194/tc-2016-112, 2016
Manuscript under review for journal The Cryosphere
Published: 6 June 2016
© Author(s) 2016. CC-BY 3.0 License.

bottom panels of Fig. 4.It suggests that the impact of assimilating SMOS-Ice leads to a reduction of sea-ice thickness both in March and November of 2014.

The time series of daily bias and RMSD for thin ice thicknesses in the OSE runs are shown in the top panels of Fig. 5. The bias of thin sea-ice thickness is reduced from 16 cm to 12 cm in March, and from 7 cm to 4 cm in November, when SMOS-Ice data is assimilated. The RMSD of thin sea ice is reduced from 35 cm to 31 cm in March, and from 27 cm to 21 cm in November. This corresponds to a reduction of the bias of 25% in March and 43% in November, and a reduction of the RMSD of about 11% in March and 22% in November. In the other panels of Fig. 5, the bias and RMSD of sea ice concentration, SST and SLA are presented. There is a slight benefit for the bias and RMSD of sea ice concentration, but the statistics for SST and SLA are unchanged.

Moreover, the time evolution of the averaged thicknesses of thin sea-ice in the marginal seas - in the Kara Sea, Barents Sea and Beaufort Sea - are highlighted with the marked lines in the panels of Fig. 6. The corresponding daily RMSDs of ice thickness relative to thin SMOS-Ice data are added with shading. In each month, there are four assimilations marked with the vertical lines.

In the Kara Sea,the thickness observed in March isvery stable with a slight gradual increase. There is a relatively uniform reduction of RMSD by about 21%, which is mainly the result from a correction of the large (too thick) bias in the model. In November, the bias is much smaller and the resulting improvement is smaller (8%) but the performances are improving slightly through the month for RMSD.

In the Barents Sea, in March, the observations show an increasing trend. The official run shows initially a large (thick) bias that is reduced as the thickness increase in the observation. Assimilation of SMOS-Ice data reduces well the initial bias, but the bias converges with the official run at the end of the month and so is the RMSD. On average, the RMSD of ice thickness is decreased about 27% from the **Test Run**. In November, the observations show large variability that is well captured in the **Official Run** but the ice is initially too thick. The RMSD reduction is about 19% from the **Test Run** compared to from the **Official Run** and both the bias and the variability seem to be reduced.

The Cryosphere Discuss., doi:10.5194/tc-2016-112, 2016
Manuscript under review for journal The Cryosphere
Published: 6 June 2016
© Author(s) 2016. CC-BY 3.0 License.

In the Beaufort Sea, there are too few observations to provide a representative estimate of the system performance in March (top panels of Fig. 4) and the statistic are not presented. In November, the observations shows an increasing trend and the official run shows once more a relatively large thick bias initially. The RMSD in the **Test Run** is reduced by about 51%，which ismainly caused by areduction of the bias. The increasing trend in the **Test Run** is in relatively well agreement with the observations.

5. Relative impact of SMOS-ice to the existing observation network

In this Section,the additional benefit of assimilating SMOS-Ice into the TOPAZ system is quantitatively compared to the standard observation network used. To do so, we evaluate a metric calculated during the analysis, the Degree of Freedom for Signal (DFS), which is now widely used for such purpose (Rodgers, 2000; Cardinali et al., 2004). During the assimilation,one can calculate the DFS as following:

$$DFS = tr\left(\frac{\partial \hat{y}}{\partial y}\right) = tr\left\{\frac{\partial [H(X^a)]}{\partial y}\right\} = tr(KH) \quad (7)$$

DFS quantifies the reduction of mode that can be attributed to each observation type. A value of DFS close to 0 means that the observation had no update, while a value of *m* means that the assimilation has reduced the number of degree of freedom of the ensemble by *m*. Note that the reduction cannot exceed the ensemble size; i.e. 100 here. In Sakov et al. (2012), it was proposed that a system should in fact not exceed 10 % of the ensemble size to avoid a collapse of the ensemble.

In Fig. 7, we are presenting the mean of the spatial DFS (Eq.8) in March and November.

$$\overline{\mathbf{DFS}}_j = \sqrt{\frac{1}{\mathbf{M}}\sum_{i=1}^{\mathbf{M}}\mathbf{DFS}_{ij}^2} \quad (8).$$

where M is the total number of assimilating times within the specific time period (here 4). In the Arctic the total DFS is dominated by the ice concentration with large value near the ice edge. The DFS for SMOS-Ice is comparatively smaller. It is larger in March than in November. However, in some region, the monthly DFS of SMOS-ice reaches value larger than 2.

The Cryosphere Discuss., doi:10.5194/tc-2016-112, 2016
Manuscript under review for journal The Cryosphere
Published: 6 June 2016
© Author(s) 2016. CC-BY 3.0 License.

Figures of 8 and 9 show the relative contribution of each observational data set calculated as follows:

$$\mathbf{RDFS_j} = 100\% \times \overline{\mathbf{DFS_j}} \bigg/ \sum_{k=1}^{O} \overline{\mathbf{DFS_k}} \quad (9).$$

where *O* is the number of the used observation types. As expected, the assimilation of ice concentration dominates the total DFS, while the impacts of SST and SLA are limited to the region that are not ice covered. Profiles in the Arctic are the ice-tethered profiles. They have a very large impact but that are very sparse. In March the SMOS-ice data has a significant impacts (> 20 % of the total DFS) in the Northern Barents Sea, the western Kara Sea, in the Baffin Bay, in the Greenland Sea and in the Hudson Bay. In November, the relative contribution is still large in the Barents Sea, the Kara Seas and the Greenland Sea, but it is now also large in the Beaufort Sea, and in the Canadian Archipelagos.

6. Summary and Discussion

The thickness observations of thin sea ice in the Arctic can be derived from SMOS brightness temperature at 1.4 GHz (Tian-Kunze, et al., 2014; Kaleschke et al., 2016). This data set is available in near real time since 2010 at daily frequency. This study investigates the impact of assimilating this data set within TOPAZ system, which is the Arctic component of the Copernicus Marine Services. It is shown that for thin ice (less than 0.4 m), TOPAZ reanalysis and the SMOS-Ice have comparable distribution, but TOPAZ reanalysis tends to overestimate thin ice thickness, especially from January to April.

We compare the benefit of assimilating SMOS-ice (thinner than 0.4) in TOPAZ system that already assimilates ice concentration, SST, SSH and temperature and salinity profiles. The comparison is carried out for two periods: February-March and October-November of 2014. The study shows that the assimilation of SMOS-Ice data reduces the thickness RMSD of thin sea-ice in March and in November by about 11% and 22% respectively, mainly caused by the reduction of the bias (too thick sea ice that seems larger in 2014 than in previous years). As in Yang et al. (2015) we find that there is slight

The Cryosphere Discuss., doi:10.5194/tc-2016-112, 2016
Manuscript under review for journal The Cryosphere
Published: 6 June 2016
© Author(s) 2016. CC-BY 3.0 License.

The Cryosphere Discussions

improvement in the ice concentration, the RMSD for SST and SLA remains unchanged but not degraded.

In this study, the DFS has been used to evaluate the relative contributions of assimilated observations to the reduction of error in TOPAZ system. The SMOS-Ice data have a smaller impact than ice concentration, but has relative high contributions in some areas.In the Greenland Sea, the Kara Sea and the Barents Sea, a significant contribution (defined as larger than 20 % of the total impact from all observations) is found both in March and November. In the Baffin Bay and Hudson Bay, the significant contributions are also found in March. In the Beaufort Sea and in the Canadian archipelagos, there is a large contribution in November.

To conclude, we found that the assimilation of SMOS-ice has an important role to reduce the thick biases at some regions for the sea ice thickness in the Arctic. It is also encouraging that the assimilation of this data set does not degrade other variables (SST, SLA, ICEC and ice drift). This suggests that SMOS-Ice can be assimilated without degradation of other skills in the operational forecasting system and included in the future runs or the extension of the reanalysis. However, further work needs to be done to better understand the uncertainty of the assimilated sea ice thickness from the SMOS-Ice. Some information, like a measure of "saturation ratio" which is defined by the relationship of the variable L-band penetration depth and the maximal retrieval thickness as a function of temperature and salinity, may be helpful for the next assimilation running.

In additional, the satellite sensor of CryoSat-2 provides data of the freeboard height can be complementary with the sensor of SMOS (Kaleschke et al., 2010). The new sea ice thicknesses derived from the combined information from SMOS and CryoSat-2 will be soon available (Kaleschke et al., 2015). Hebert et al. (2016) presented a blended sea ice thickness from Cryosat-2 and SMOS, in which the thicknesses thinner than 0.45 m are kept from SMOS. The blended sea ice thickness has been implemented into the U.S Navy Arctic Cap Nowcast/Forecast System (ACNFS) for one year. This kind combined observations for sea ice thickness may provide more reliable estimates, and give more potential abilities to improve the forecast performance in an operational ocean system by data assimilation.

The Cryosphere Discuss., doi:10.5194/tc-2016-112, 2016
Manuscript under review for journal The Cryosphere
Published: 6 June 2016
© Author(s) 2016. CC-BY 3.0 License.

The Cryosphere Discussions
Open Access
EGU

Acknowledgment

This study was supported by the projects (ESA contracts 4000101476/10/NL/CT and 4000112022/14/I-AM) and the CPU time from the Norwegian Supercomputing Project (NOTUR II grant number nn2993k).

Reference:

Bentsen, M., Evensen, G., Drange, H., and Jenkins, A. D.: Coordinate transformation on a sphere using conformal mapping, Mon. Weather Rev., 127, 2733–2740, doi:http://dx.doi.org/10.1175/1520-0493(1999)127<2733:CTOASU>2.0.CO:2, 1999.

Bleck, R.: An oceanic general circulation model framed in hybrid isopycnic-Cartesian coordinates, Ocean Model., 4, 55–88, doi:10.1016/S1463-5003(01)00012-9, 2002.

Bouillon, S., Fichefet, T.,Legat, V., and Madec, G.: The elastic-viscous-plastic method revised. Ocean Modell. 7, 2-12.doi:10.1016/j.ocemod.2013.05.013, 2013.

Cardinali, C., Pezzulli, S., and Andersson, E.: Influence-matrix di- agnostic of a data assimilation system, Q. J. R. Meteorol. Soc., 130, 2767–2786, doi:10.1256/qj.03.205, 2004.

Chapman, W.L., and Walsh, J. E.: Recent variations of sea ice and air temperature in high latitudes, Bull. A mer. Meteorol. Soc., 74, 33 —47, doi: http://dx.doi.org/10.1175/1520-0477(1993)074<0033:RVOSIA>2.0.CO:2, 1993.

Chassignet, E. P., Hurlburt, H. E., Metzger, E. J., Smedstad, O. M., Cummings, J., Halliwell, G. R., Bleck, R., Baraille, R., Wallcraft, A. J., Lozano, C., Tolman, H. L., Srinivasan, A., Hankin, S., Cornillon, P., Weisberg, R., Barth, A., He, R., Werner, F., and Wilkin, J.: US GODAE: Global Ocean Prediction with the HYbrid Coordinate Ocean Model (HYCOM), Oceanography, 22, 64–75. Doi:10.5670/oceanog.2009.39, 2009.

Chassignet, E. P., Smith, L. T., and Halliwell, G. R.: North Atlantic Simulations with the Hybrid Coordinate Ocean Model (HYCOM): Impact of the vertical coordinate choice, reference pressure, and termobaricity, J. Phys. Oceanogr., 33, 2504–2526. Doi: http://dx.doi.org/10.1175/1520-0485(2003)033<2504:NASWTH>2.0.CO:2, 2003.

Connor, L. N., Laxon, S. W.,Ridout, A. L., Krabill, W. B.,and McAdoo, D. C.: Comparison of Envisat radar and airborne laser altimeter measurement over Arctic sea ice. Remote Sensing of Environment. 113, 563-570, dio:10.1016/j.rse.2008.10.015, 2009

Dee, D.P., Uppala, S. M., Simmons, A. J.,Berrisford, P., et al.: The ERA-Interim reanalysis: configuration and performance of the data assimilation system, Quart. J. Roy. Meteor. Soc., 137, 553–597.Doi: 10.1002/qj.828, 2011

Donlon, C.J., Martin, M., Stark, J. D., Roberts-Jones, J., and Fiedler, E.: The Operational Sea Surface Temperature and Sea Ice Analysis (OSTIA) system. Rem. Sens. of Environment, 116: 140-158. doi:10.1016/j.rse.2010.10.017, 2012.

Drange, H., and Simonsen, K.: Formulation of air-sea fluxes in the ESOP2 version of MICOM, Technical Report No. 125 of Nansen Environmental and Remote Sensing Center, 1996.

Forsberg, R. and Skourup, H.: Arctic Ocean gravity, geoid and sea-ice freeboard heights from ICESat and GRACE. *Geophys. Res. Lett.*,**32**(21), L21502. doi:10.1029/2005GL023711, 2005.

Giles, K. A., Laxon, S. W.,Wingham, D. J., et al.: Combined airborne laser and radar altimeter measurements over the Fram Strait in May 2002. Remote Sensing of Environment. 111(2-3), 182-194, doi:10.1016/j.rse.2007.02.037, 2007.

Giles, K. A., Laxon, S. W., and Ridout, A. L.: Circumpolar thinning of Arctic sea ice following the 2007 record ice extent minimum, Geophys. Res. Lett., 35, L22502, doi:10.1029/ 2008GL035710, 2008.

Guemas, V., Wrigglesworth, E. B., Chevallier, M., et al.: A review on Arctic

1

The Cryosphere Discuss., doi:10.5194/tc-2016-112, 2016
Manuscript under review for journal The Cryosphere
Published: 6 June 2016
© Author(s) 2016. CC-BY 3.0 License.

sea- icepredictability and prediction on seasonal to decadal timescales. Q. J. R. Meteorolog. Soc., 142(695), dio:10.1002/qj.2401, 2014.

Hebert, D., Posey, P., Allard, R. Wallcraft, A., Metzger, E. J., and Li, L.: High resolution sea ice data assimilation and verification in the U.S. Navy Arctic Cap Nowcast/Forecast System 30 (ACNFS) and Global Ocean Forecast System (GOFS) 3.1, 7th IICWG Data assimilation and PPP ice verification Workshop, Frascati, Italy. 2016.

Heygster, G., Hendricks, S., Kaleschke, L., Maass, N., Mills, P., Stammer, D., Tonboe, R. T.,and Haas, C.:*L-Band Radiometry for Sea-Ice Applications*, Final Report for ESA ESTEC Contract 21130/08/NL/EL, Institute of Environmental Physics, University of Bremen, November 2009, 219 pp, 2009.

Hunke, E. C., and Dukowicz, J. K.: An elastic-viscous-plastic model for sea ice dynamics, J. Phys. Oceanogr., 27, 1849–1867. Doi: http://dx.doi.org/10.1175/1520-0485(1997)027<1849:AEVPMF>2.0.CO:2, 1997.

Huntemann, M., Heygster, G., Kaleschke, L., Krumpen, T., Mäkynen, M., and Mrusch, M.: Empirial sea ice thickness retrieval during the freeze-up period from SMOS high incident angle observations, The Cryosphere, 8, 439-451, doi:10.5194/tc-8-439-2014, 2014

Kaleschke, L., Maaß, N., Haas, C., Hendricks, S., Heygster, G., and Tonboe, R.: A sea-ice thickness retrieval model for 1.4 GHz radiometry and application to airborne measurements over low salinity sea-ice, The Cryosphere, 4, 583 – 592. Doi: 10.5194/tc-4-583-2010, 2010.

Kaleschke, L., Tian-Kunze, X., Maaß, N., Mäkynen, M., and Drusch, M.: Sea ice thickness retrieval from SMOS brightness temperatures during the Arctic freeze-up period. J. Geophys. Lett. 39, L05501, doi: 10.1029/2012GL050916, 2012

Kaleschke, L., Tian-Kunze, X., Maaß, N., Ricker, R., Hendricks, S., and Drusch, M.: Improved retrieval of sea ice thickness from SMOS and Cryosat-2. Proceedings of 2015 International Geoscience and Remote Sensing Symposium IGARSS. Doi: 10.1109/IGARSS.2015.7327014, 2015.

Kaleschke, L., Tian-Kunze, X., Maaß, N., et al.: SMOS sea ice product: Operational application and validation in the Barents Sea marginal ice zone. Remote Sensing of Environment, doi:10.1016/j.rse.2016.03.009, 2016.

Karl, T. R., Arguez, A., Huang, B., Lawrimore, J. H., McMahon, J. R., Menne, M. J., Peterson, T. C., Vose, R. S., and Zhang, H.-M.: Possible artifacts of data biases in the recent global surface warming hiatus. Science, 348 (6242), 1469-1472.doi: 10.1126/science.aaa5632, 2015.

Korosov, A., Counillon, F., and Johannessen, J. A.: Monitoring the spreading of the Amazon freshwater plume by MODIS, SMOS, Aquarius, and TOPAZ. J .Geophys. Res., 120, 268-283, doi:10.1002/2014JC010155, 2015.

Kurtz, N. T., Markus, T., Cavalieri, D. J., Sparling, L. C., Krabill, W. B., Gasiewski, A. J., and Sonntag, J. G.: Estimation of sea ice thickness distributions through the combination of snow depth and satellite laser altimetry data, J. Geophys. Res., 114, C10007, doi:10.1029/2009JC005292, 2009.

Kurtz, N. T., Farrell, S. L.,Studinger, M., Galin, N., Harbeck, J. P., Lindsay, R.,Onana, V. D., Panzer, B., and Sonntag, J. G.: Sea ice thickness, freeboard, and snow depth products from Operation IceBridge airborne data. The Cryosphere 7: 1035-1056. doi:10.5194/tc-7-1035-2013, 2013.

Kwok, R., and Rothrock, D.: Decline in Arctic sea ice thickness from submarine and ICESat records: 1958–2008, Geophys. Res. Lett., 36, L15501, doi:10.1029/2009GL039035, 2009.

Johnson, M., Proshutinsky A., Aksenov Y., Nguyen A. T., Lindsay R., Haas C., Zhang J., Diansky N., Kwok R., et al.: Evaluation of Arctic sea ice thickness simulated by Arctic Ocean Model Intercomparison Project models. J.Geophys. Res., 117(C8), doi:10.1029/2011JC007257, 2012.

Johannessen, J. A., Raj, R.P.,Nilesen, J. E. Ø., Pripp, T., Knudsen, P., Counillon, F., Stammer, D., Bertino, L., Andersen, O. B., Serra, N., and Koldunov, N.: Toward Improved Estimation of the Dynamic Topography and Ocean Circulation in the High Latitude and Arctic Ocean: The Importance of GOCE. SurvGeophys, doi:10.1007/s10712-013-9270-y,

© Author(s) 2016. CC-BY 3.0 License.

2014.
Johannessen, O. M., Shalina, E. V., and Miles, M. W.: Satellite evidence for an Arctic Sea ice cover in transformation, Science, 286, 1937—1939. Doi:10.1126/science.286.5446.1937, 1999.
Laxon, S., Peacock, N., and Smith, D.: High interannualvariabilityof sea ice thickness in the Arctic region, Nature, 425, 947–950, doi:10.1038/nature02050, 2003.
Laxon, S. W., Giles, K. A., Ridout, A. L., Wingham, D. J., Willatt, R., Cullen, R., Kwok, R., Schweiger, A., Zhang, J., Haas, C., Hendricks, S., Krishfield, R., Kurtz, N., Farrell, S., and Davidson, M.: CryoSat-2 estimates of Arctic sea ice thickness and volume, Geophys. Res. Lett., 40, 732–737, doi:10.1002/grl.50193, 2013.
Lien, V. S., Hjøllo, S. S., Skogen, M. D.,,Svendsen, E., Wehde, H., Bertino, L., Counillon, F., Chevallier, M., and Garric, G.: An assessment of the added value from data assimilation on modelled Nordic Seas hydrography and ocean transports, Ocean Modelling, doi:10.1016/j.ocemod.2015.12.010, 2016.
Locarnini, R., Antonov, J., and Garcia, H.: World Ocean Atlas 2005, Volume 1: Temperature., vol. 61, US Dept. of Commerce, National Oceanic and Atmospheric Administration, 2006.
Mecklenburg, S., Drusch, M., Kaleschke, L., Rodriguez-Fernandez, N., Reul, N., Kerr, Y., Font, J., Martin-Neira, M., Oliva, R., Daganzo-Eusebio, E., Grant, J. P., Sabia, R., Macelloni, G., Rautiainen, K., Fauste, J., de Rosnay, P., Munoz-Sabater, J., Verhoest, N., Lievens, H., Delwart, S., Crapolicchio, R., de la Fuente, A., and Kornberg, M.: ESA's Soil Moisture and Ocean Salinity mission: From science to operational applications, Remote Sensing of Environment, http://dx.doi.org/10.1016/j.rse.2015.12.025, 2016.
Melsom, A., Counillon, F., LaCasce, J. H., and Bertino, L.: Forecasting search areas using ensemble ocean circulation modeling. Ocean Dynamics, 62(8), 1245-1257, 2012.
Outten, S. andEsau, I.: A link between Arctic sea ice and recent cooling trends over Eurasia, Climatic Change, 110, 1069–1075, doi:10.1007/s10584-011-0334-z, 2012.
Ricker, R., Hendricks, S., Helm, V., et al.: Sensitivity of CryoSat-2 Arctic sea-ice freeboard and thickness on radar-waveform interpretation, The Cryosphere, 8, 1607-1622, doi:10.5194/tc-8-1607-2014, 2014.
Rodgers, C.: Inverse methods for atmospheres: theory and practice, World Scientific, 2000.
Roemmich, D., Church, J., Gilson, J., Monselesan, D., Sutton, P., and Wijffels, S.: Unabated planetary warming and its ocean structure since 2006. *Nature Climate Change*5, 240–245. doi:10.1038/nclimate2513, 2015.
Rothrock, D.A., Yu, Y., and Maykut, G. A.: Thinning of the Arctic sea ice cover, Geophys. Res. Lett r., 26, 3469 —3472. Doi:10.1029/1999GL010863, 1999.
Sakov, P., and Oke, P. R.: A deterministic formulation of the ensemble Kalman _lter: an alternative to ensemble square root filters. Tellus A, 60(2):361-371, doi:10.1111/j.1600-0870.2007.00299.x, 2008.
Sakov, P., Evensen, G., and Bertino, L.: Asynchronous data assimilation with the EnKF. Tellus A, 62(1), 24-29. Doi:10.1111/j.1600-0870.2009.00417.x, 2010.
Sakov, P., Counillon, F., Bertino, L., Lisæter, K. A., Oke, P. R., and Korablev, A.: TOPAZ4: an ocean-sea ice data assimilation system for the North Atlantic and Arctic. Ocean Science, 8:633-656, doi:10.5194/os-8-633-2012, 2012.
Schweiger, A., Lindsay, R., Zhang, J., Steels, M., Stern, H., and Kwok, R.: Uncertainty in modeled Arctic sea ice volume, J. Geophys. R., 116, C00D06, doi:10.1029/2011JC007084, 2012.
Screen, J. A., and Simmonds, I.: Declining summer snowfall in the Arctic: Causes, impacts and feedbacks, Clim. Dynam., 38, 2243–2256, doi:10.1007/s00382-011-1105-2, 2012.
Serreze, M., Walsh, J., Chapin, F., Osterkamp, T., Dyurgerov, M., Romanovsky, V., Oechel, W., Morrison, J., Zhang, T., and Barry, R. G.: Observational evidence of recent changes in the northern high latitude environment, Climate Change, 46,159 —207. Doi: 10.1023/A:1005504031923, 2000.
Shimada, K., Kamoshida, T., Itoh, M., Nishino, S., Carmack, E., McLaughlin, F., Zimmermann, S., and Proshutinsky, A.: Pacific Ocean inflow: Influence on catastrophic reduction of sea ice cover in the Arctic Ocean, Geophys. Res. Lett., 33(8),

The Cryosphere Discuss., doi:10.5194/tc-2016-112, 2016
Manuscript under review for journal The Cryosphere
Published: 6 June 2016
© Author(s) 2016. CC-BY 3.0 License.

doi:10.1029/2005GL025624, 2006.

Simmons, A., Uppala, S., Dee, D., and Kobayashi, S.: ERA-Interim: New ECMWF reanalysis products from 1989 onwards, ECMWF Newsletter, 110-Winter 2006/07, 25-35, 2007.

Smith, G. C., Roy, F., Reszka, M., Colan, D. S., He, Z., Deacu, D., et al.: Sea ice forecast verification in the Canadian Global Ice Ocean Prediction System. Quart. J. Roy. Meteor. Soc., doi:10.1003/qj.2555, 2015.

Steele, M., Morley, R., and Ermold, W.: PHC: A global ocean hydrography with a high-quality Arctic Ocean, J. Climate, 14, 2079–2087. Doi:http://dx.doi.org/10.1175/1520-0442(2001)014<2079:PAGOHW>2.0.CO:2, 2001.

Tian-Kunze, X., Kaleschke, L., Maaß, N., Mäkynen, M., Serra, N., Drusch, M., and Krumpen, T.: SMOS-derived sea ice thickness: algorithm baseline, product specifications and initial verification, The Cryosphere, 8, 997-1018, doi:10.5194/tc-8-997-2014, 2014.

Tilling, R. L., Ridout, A., and Shepherd, A.: Near real time Arctic sea ice thickness and volume from CryoSat-2, The Cryosphere Discuss., doi:10.5194/tc-2016-21, 2016.

Vandenbulcke, L., and Barth, A.: A stochastic operational forecasting system of the Black Sea: Technique and validation. Ocean Modell., 93, 7-12, doi:10.1016/j.ocemod.2015.07.010, 2015.

Winther, N.G., and Evensen, G.: A hybrid coordinate ocean model for shelf sea simulation. Ocean Modell., 13, 221–237.Doi: 10.1016/j.ocemod.2006.01.004, 2006.

Woodgate, R. A., Weingartner, T. J., and Lindsay, R.: Observed increases in Bering Strait oceanic fluxes from the Pacific to the Arctic from 2001 to 2011 and their impacts on the Arctic Ocean water column, Geophys. Res. Lett., 39, L24603, doi:10.1029/2012GL054092, 2012.

Xie, J., Bertino, L.,Counillon, F., Lisæter, K. A., and Sakov, P.: Quality assessment of the TOPAZ4 reanalysis in the Arctic over the period 1991-2013, 2016 (Submitted)

Yang, Q., Losa, S. N., Losch, M., Tian-Kunze, X., Nerger, L., Liu, J., Kaleschke, L., and Zhang, Z.: Assimilating SMOS sea ice thickness into a coupled ice-ocean model using a local SEIK filter, J. Geophys. Res. Oceans, 119, doi:10.1002/2014JC009963, 2014.

Zygmuntowska, M., Rampal, P., Ivanova, N., and Smedsrud, L. H.: Uncertainties in Arctic sea ice thickness and volume: new estimates and implications for trends. The Cryosphere, 8, 705–720, doi:10.5194/tc-8-705-2014, 2014.

The Cryosphere Discuss., doi:10.5194/tc-2016-112, 2016
Manuscript under review for journal The Cryosphere
Published: 6 June 2016
© Author(s) 2016. CC-BY 3.0 License.

The Cryosphere Discussions Open Access EGU

Table 1. Overview of assimilated observations in each assimilation cycle of the present TOPAZ system. All observations are retrieved from http://marine.copernicus.eu.

Type	Spacing	Resolution	Provider
SLA	Track	-	CLS
SST	Gridded	5 km	OSTIA from UK Met Office
In-situ T	Point	-	Ifremer + other
In-situ S	Point	-	Ifremer + other
ICEC	Gridded	10 km	OSISAF
Ice drift	Gridded	62.5 km	OSISAF

© Author(s) 2016. CC-BY 3.0 License.

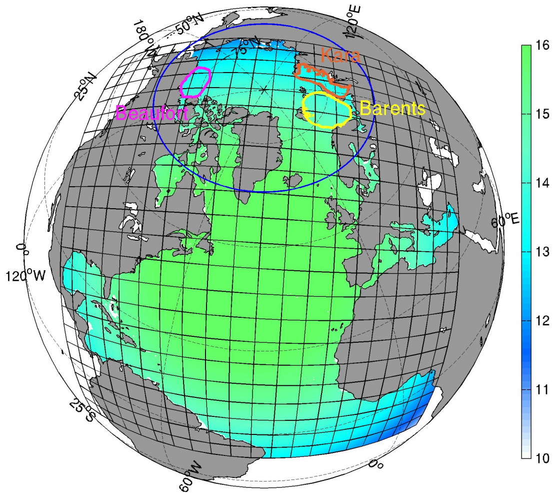

Fig. 1 TOPAZ model domain and horizontal grid resolution (km) with color shading. The blue line delimits the focused Arctic region (north of 63°N) and other color lines delimit the three marginal seas discussed in this study.

The Cryosphere Discuss., doi:10.5194/tc-2016-112, 2016
Manuscript under review for journal The Cryosphere
Published: 6 June 2016
© Author(s) 2016. CC-BY 3.0 License.

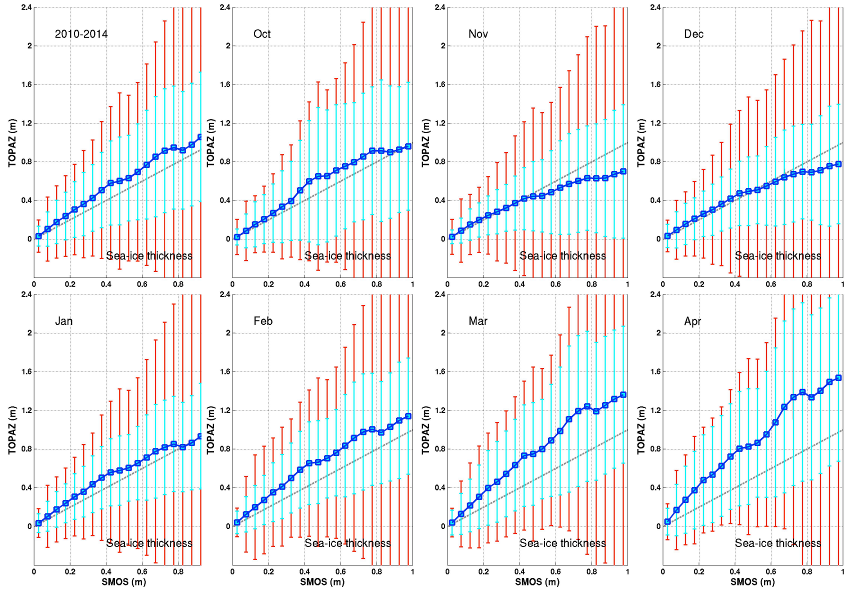

Fig. 2 Conditional expectations of TOPAZ versus SMOS-Ice (with bin of 5 cm) for the period 2010-2014 and for each month.The cyan error-bars correspond to the RMSD against all observations within each bin. The red error-bars correspond to averaged standard deviations of observation error. The gray dashed line denotes the line y=x.

The Cryosphere Discuss., doi:10.5194/tc-2016-112, 2016
Manuscript under review for journal The Cryosphere
Published: 6 June 2016
© Author(s) 2016. CC-BY 3.0 License.

The Cryosphere Discussions
Open Access

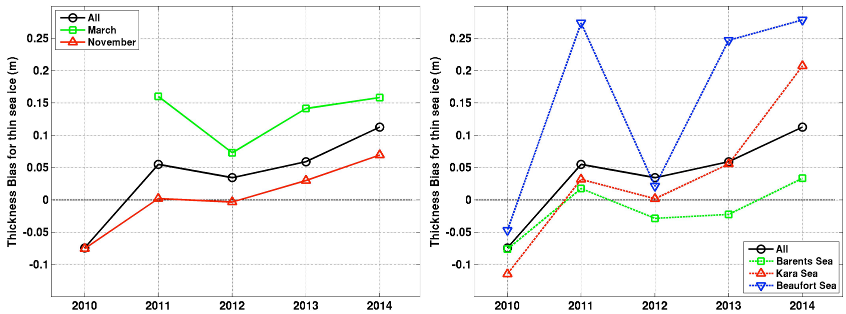

Fig. 3 Yearly thickness biases of thin sea ice from TOPAZ compared to SMOS-Ice observations. The black line represents the yearly mean bias. **Left**: the green (resp. red) line represents the mean bias for March (resp. November) of each year. **Right**: the colored lines represent the mean biases in the Barents Sea, the Kara Sea, and the Beaufort Sea.

The Cryosphere Discuss., doi:10.5194/tc-2016-112, 2016
Manuscript under review for journal The Cryosphere
Published: 6 June 2016
© Author(s) 2016. CC-BY 3.0 License.

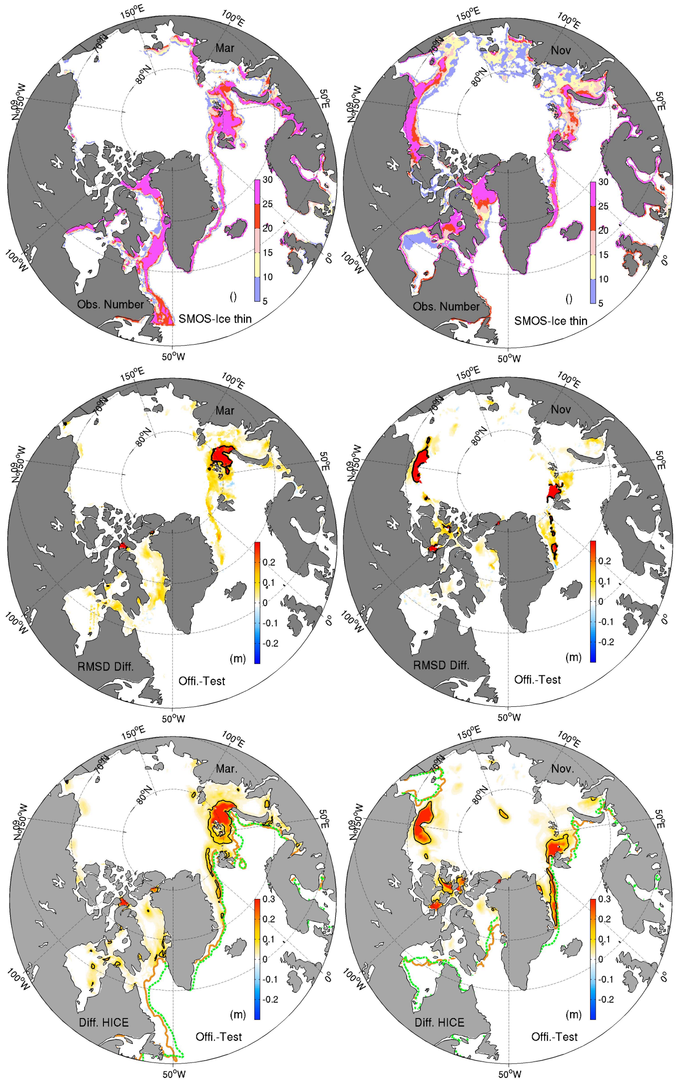

Fig. 4 **Top**: SMOS-Ice data assimilated in the modelin March (left) and in November (right). **Middle**: Difference of RMSDs forthe thin sea-ice thicknesses between the **Official Run** and the **Test Run** in March (*left*) and in November (*right*). **Bottom:** Difference of mean ice thicknesses between the two runs. The black line denotes the 0.2 m isoline, the green (resp. orange) line is the 15% concentration isoline from OSISAF (resp. the **Official Run**).

The Cryosphere Discuss., doi:10.5194/tc-2016-112, 2016
Manuscript under review for journal The Cryosphere
Published: 6 June 2016
© Author(s) 2016. CC-BY 3.0 License.

The Cryosphere
Discussions
Open Access

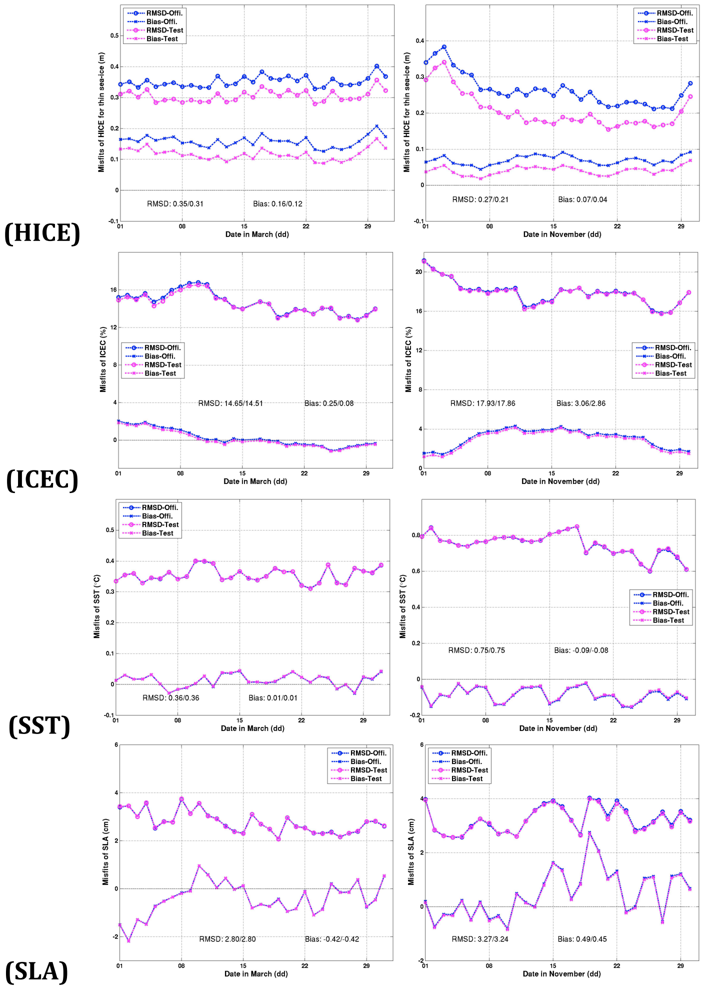

Fig. 5 Daily time series of the bias (marked with crosses) and the RMSD (marked with circles) in the whole Arctic for the **Official Run** (in blue) and the **Test Run** (in purple) for different variables in March (Left) and November (Right).

© Author(s) 2016. CC-BY 3.0 License.

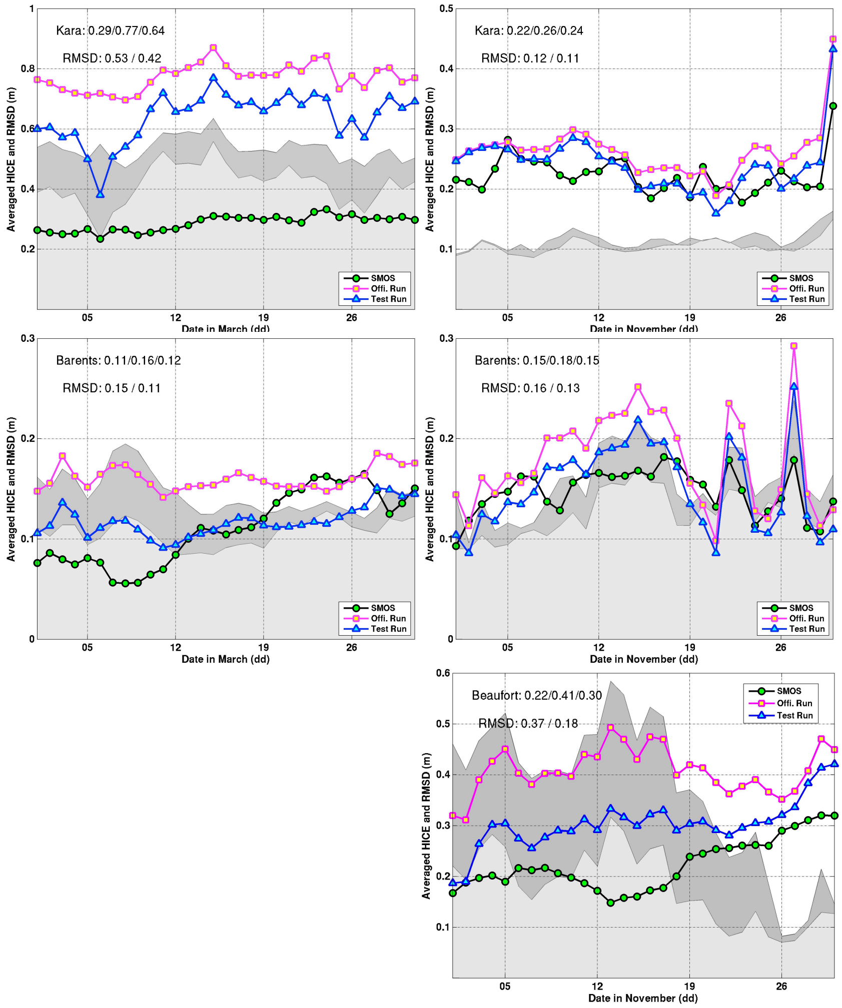

Fig. 6 Daily time series of the mean thickness of thin sea-ice in the Kara Sea (upper), the Barents Sea (middle) and Beaufort Sea (bottom) for March (*left*) and November (*right*). The light (resp. dark) gray shading is the dailyspatial RMSD of thin sea ice in the **Test Run** (resp. **Official Run**).

The Cryosphere Discuss., doi:10.5194/tc-2016-112, 2016
Manuscript under review for journal The Cryosphere
Published: 6 June 2016
© Author(s) 2016. CC-BY 3.0 License.

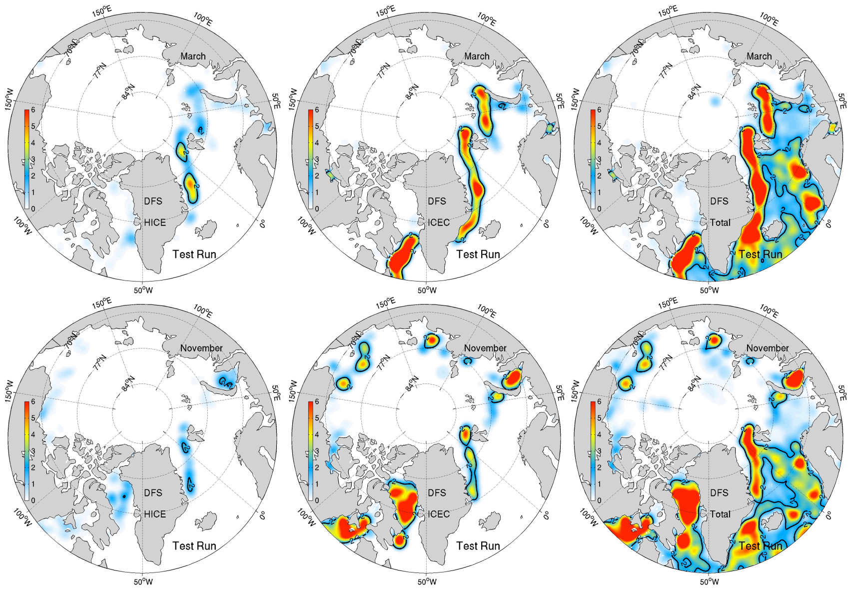

Fig. 7 Monthly averaged Degrees of Freedom for Signal (DFS) from the **Test Run** in March (*upper*) and in November (*lower*) for SMOS-Ice sea ice thickness (left), sea ice concentration (middle), and the total DFS of all ice and ocean observations (right). The black line denotes the isoline of DFS equal to 2.

The Cryosphere Discuss., doi:10.5194/tc-2016-112, 2016
Manuscript under review for journal The Cryosphere
Published: 6 June 2016
© Author(s) 2016. CC-BY 3.0 License.

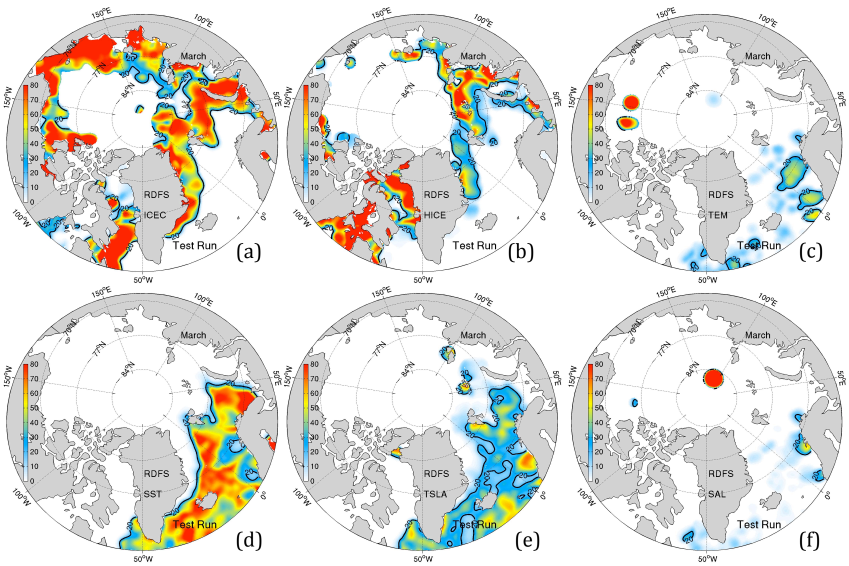

Fig. 8 Relative contributions of each observational data set in the total DFS during March 2014. Panel (a) is for sea ice concentration; (b) ice thickness from SMOS-Ice; (c) temperature profiles; (d) SST; (e) along-track SLA; (f) salinity profiles. The black line is the 20% isoline.

The Cryosphere Discuss., doi:10.5194/tc-2016-112, 2016
Manuscript under review for journal The Cryosphere
Published: 6 June 2016
© Author(s) 2016. CC-BY 3.0 License.

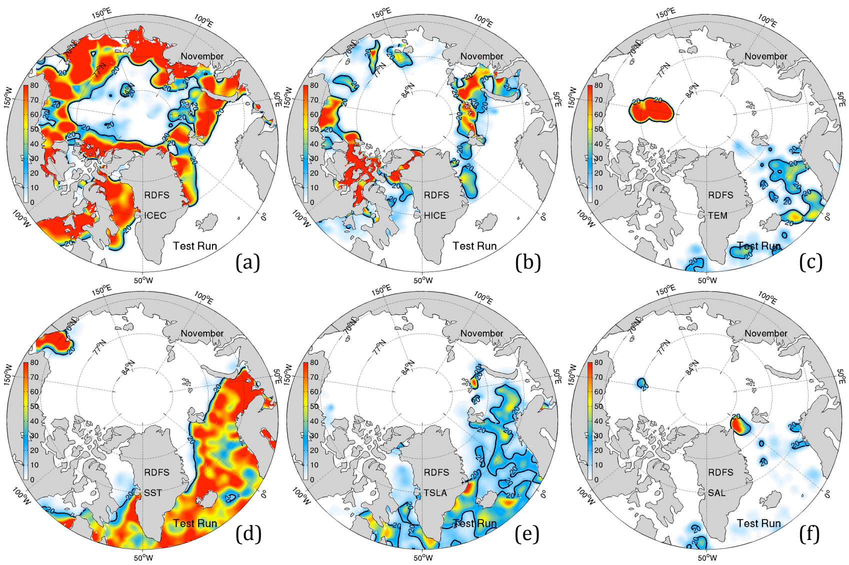

Fig. 9 Same as Figure 8 for November 2014